

1 **EVALUATION OF A SPLICE CONNECTION FOR PRECAST CONCRETE PILES**

2  
3 **Mikayla Bladow, EIT, PES Structural Engineers, Atlanta, GA**  
4 **Brandon E. Ross, PhD, PE, Clemson University, Clemson, SC**  
5 **Thomas E. Cousins, PhD, PE, Clemson University, Clemson, SC**  
6 **Mahmoodreza Soltani, EIT, PhD Candidate, Clemson, SC**  
7  
8

9 **ABSTRACT**

10  
11 *Two flexural tests were performed for a connection for splicing precast concrete piles. The*  
12 *splice consisted of steel male studs and female sockets attached with steel locking pins.*  
13 *Internal forces in the splice were transmitted to the piles through #10 bars welded to the*  
14 *back side of the splice assemblies. The splice connection exhibited experimental flexural*  
15 *capacities of 273 kip-foot and 287 kip-feet. Peak capacities corresponded to crushing of the*  
16 *concrete compression zone adjacent to the splice location. This report presents details of the*  
17 *test program and theoretical calculations of flexural capacity. Comparison between*  
18 *experimental and theoretical results suggest that the #10 bars were near ultimate capacity at*  
19 *peak load.*  
20  
21

22 **Keywords:** Connections, Testing, Flexural Capacity, Piles  
23  
24  
25  
26  
27  
28  
29  
30  
31  
32  
33  
34  
35  
36  
37  
38  
39  
40  
41  
42  
43  
44

45

46 **INTRODUCTION**

47

48 Due to fabrication, transportation, and handling constraints, it is common to build precast  
 49 concrete piles from multiple pile segments. Splice connections between the segments must  
 50 be capable of transmitting axial and flexural loads. Rapidity of construction is another  
 51 primary concern when designing and specifying splice connections. This paper presents  
 52 details of testing and analysis of a splice connection. The work was conducted to evaluate the  
 53 splice connection for compliance with flexural strength requirements of the Florida  
 54 Department of Transportation (FDOT) *Standard Specifications for Road and Bridge*  
 55 *Construction*<sup>1</sup>. FDOT requires that mechanical splice connections for 18 inch x 18 inch piles  
 56 be cable of resisting 245 kip-ft of moment, which is approximately equal to the design  
 57 flexural strength of the pile at sections away from the splice.

58

59 **PILE AND SPLICE DETAILS**

60

61 Two specimens were tested. Each test specimen consisted of two 18 inch x 18 inch x 20 foot  
 62 long prestressed concrete pile segments. The segments were fabricated in July 2015 by a  
 63 precaster in the Southeastern US according to standard pile details from the FDOT<sup>2</sup>. After  
 64 fabrication the segments were trucked to Clemson University where they were spliced and  
 65 tested. Material properties for the piles are presented in Table 1.

66

67 Table 1 - Material properties of piles

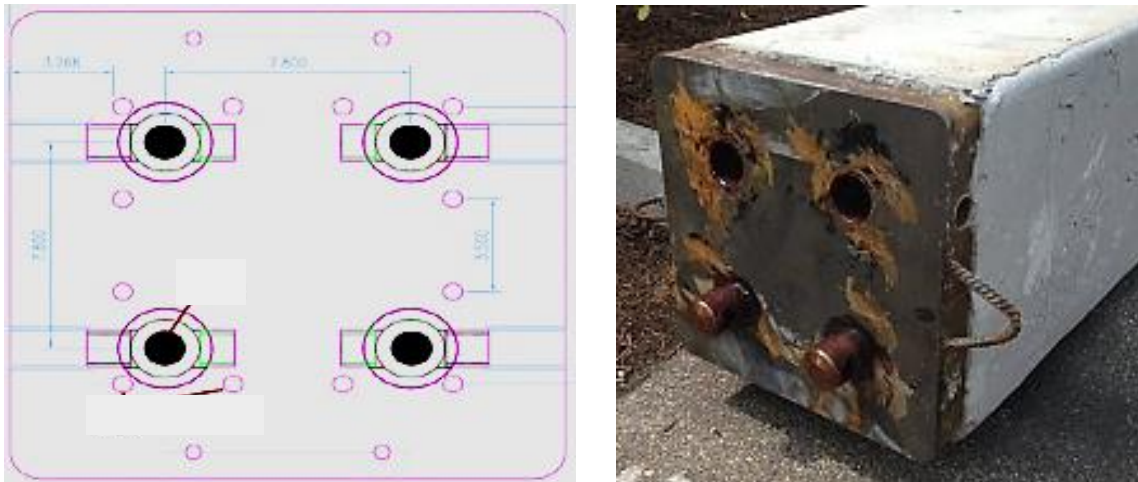
<b>Material</b>	<b>Specified minimum strength (ksi)</b>	<b>*Tested Strength (ksi)</b>
Concrete	6	7.7
Prestressing strand	270	NP
Spiral reinforcement wire	80	NP
**Auxiliary reinforcement	70	NP
*Based on test results and documentation provided by precaster; NP: not provided		
**Does not include #10 bars attached to splice assembly		

68

69 The FDOT Standard Specifications for Road and Bridge Construction<sup>2</sup> require that  
 70 mechanical splice connections be cable of resisting 245 kip-ft for 18 inch x 18 inch piles.  
 71 The splice is made by connecting steel assemblies placed at the end of each pile segment  
 72 during fabrication (Fig. 1). Each assembly is comprised of #10 bars, male studs, female  
 73 sockets, pines, and a cap plate. The #10 bars are welded to the back of the studs and sockets.  
 74 Material properties of the splice assembly components are summarized in Table 2.

75

76



77  
78 Fig. 1 –Pile Splice Connection

79  
80 The steel assembly on each side of the splice contains both the male and female components.  
81 This can be seen in Fig. 1 wherein the assembly in the picture has male studs at the bottom  
82 and female sockets at the top. This arrangement is reversed on the opposite assembly. By  
83 detailing the assemblies in this manner, the assemblies are interchangeable.

84  
85 Working left-to-right in Fig. 2, the load path through the splice connection is as follows:  
86 Flexural-tension force from the pile is transferred to #10 bars, which are welded to the back  
87 of the socket. Forces are transferred between the socket and stud through a locking pin which  
88 is inserted from the side after the two splice assemblies are joined. A #10 bar is welded to the  
89 back side of the stud to receive forces from the stud and deliver them to the pile. The #10  
90 bars extend four feet into each pile.

91  
92 Flexural-tension forces are carried by prestressing strands beyond the termination point of the  
93 #10 bars. During fabrication, the prestressing strands extended through holes in the cap  
94 plates. Strands were cut flush with the surface of the cap plate by the pile fabricator, but  
95 were not connected to the splice assembly. Yielding of the #10 bars was designed to be the  
96 controlling limit state for flexural-tension forces.

97  
98 The piles were oriented horizontally end-to-end on the ground during the splicing process.  
99 One of the segments was supported on wood dunnage and the other was supported by a crane  
100 (Fig. 3). In order to get the locking pins to fit into the holes, the cap plates needed to be flush  
101 against each other. This required some adjustments to the crane-supported pile segment.  
102 Once aligned, the pins required 10-12 hits with a 2 lb hammer to be secured in place (Fig. 4).  
103 The time from when that the segments were oriented end-to-end (Fig. 3) until the locking  
104 pins were secured in place was approximately 10 minutes. After the segments were spliced,  
105 they were lifted by crane to the testing bed (Fig. 5).

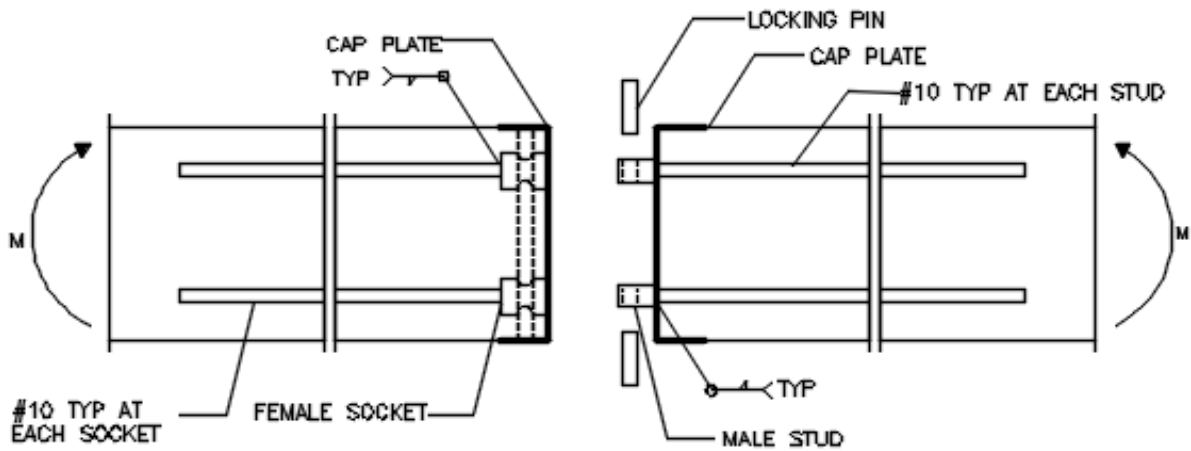
106  
107 In practice the pile segments would be oriented vertically during the splicing process. This  
108 would likely decrease the effort and time required to complete the splice because gravity  
109 would pull the cap plates flush, which would also align the holes for the locking pins.

110 Table 2 - Splice material properties

Component	Specification	*F <sub>y</sub> (ksi)	*F <sub>u</sub> (ksi)
Locking Pin	ASTM A311	100	115
Male Stud	EN S355 J2G3	51.5	91
Female Socket	EN S355 J2G3	51.1	74
#10 bars	ASTM A706	72 (82 tested)**	90 (110 tested)**
Weld Metal	AWS ER80S-X	65	80
Cap Plate	ASTM A572-Gr50	50	65

\*All properties are specified properties unless otherwise noted.  
 \*\*Based on test data provided by bar supplier

111  
112  
113



Notes:

- Prestressing strands not shown for clarity
- #10 bars extend 4' from back of stud/socket

114  
115  
116  
117  
118

Fig. 2 – Components in Pile Splice Connection



119  
120 Fig. 3 - Pile supported by crane and wood dunnage  
121

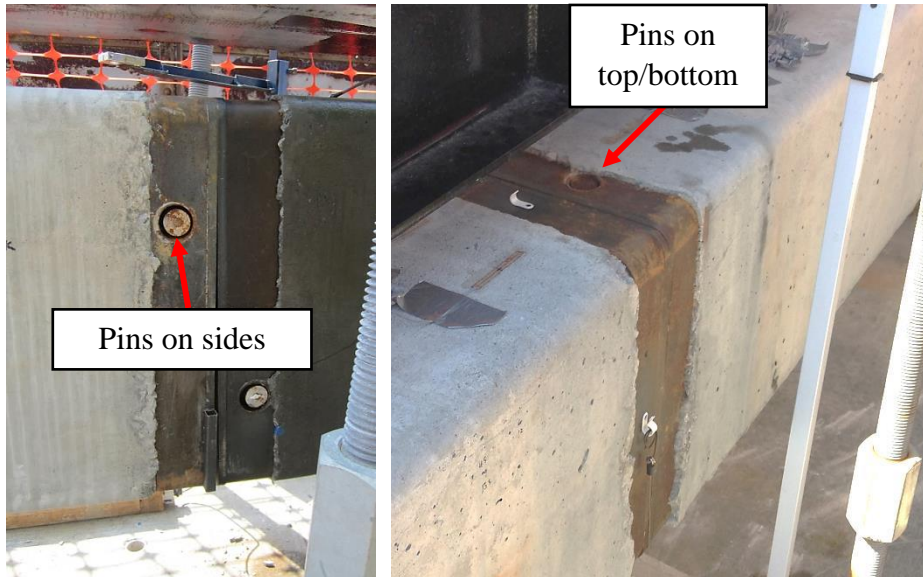


122  
123 Fig. 4 – Splice connection during alignment (left) and installation of locking pins (right)  
124



125  
126 Fig. 5 – Segments spliced together and positioned on test bed  
127

128 Two test specimens were built from four pile segments. The specimens were effectively  
129 identical. The only difference between the specimens was orientation of the pins during  
130 testing. Pins were located on the sides for Test 1 (Fig. 6 left) and on the top/bottom for Test  
131 2 (Fig. 6 right). For piles supporting a bridge or other structure, flexural moments in the piles  
132 can be applied to the splice along either or both axes. For this reason, both orientations were  
133 tested in the experiments.  
134



135  
136 Fig. 6- Pin orientations for Test 1 (left) and Test 2 (right)

137

138

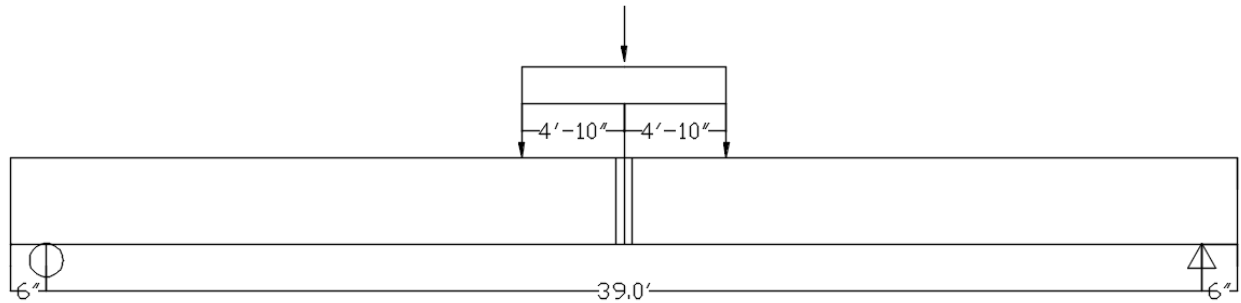
### 139 TEST SETUP

140

141 As shown in Fig. 5 and Fig. 7, the specimens spanned horizontally and were supported at  
142 each end. The splice was located at mid-span. Load was applied through a steel spreader  
143 beam that was centered over the splice. A hydraulic actuator applied load to the center of the  
144 spreader beam (Fig. 8). Pressure in the hydraulic system was monitored and recorded during  
145 testing using an electronic pressure gauge. The applied force was calculated by multiplying  
146 the gauge pressure by the internal cross-sectional area of the jack. The pressure gauge was  
147 calibrated prior to testing and found to be accurate to within +/- 0.5%.  
148

149





150  
151  
152

Fig. 7 – Support and load geometry

153  
154



155  
156  
157

Fig. 8 – Hydraulic jack and spreader beam

158 String potentiometers were placed on both sides of the specimen at the splice location to  
 159 measure mid-span vertical displacement during testing. Displacements were effectively  
 160 identical for each side, indicating that the piles did not rotate during testing. Displacement  
 161 was also measured periodically during testing using a tape measure; the tape measure  
 162 readings were consistent with those reported by the string potentiometers.  
 163  
 164  
 165  
 166

167 **TEST RESULTS**

168

169 The specimens supported peak moments of 273 kip-feet and 287 kip-feet for Test 1 and Test  
170 2, respectively. These values include moment from both self-weight and applied load.  
171 Moment-displacement responses of the piles are presented in Fig. 9. The target moment  
172 based on FDOT requirements ( $M_{target}$ ), calculated nominal moment ( $M_n$ ), and calculated  
173 upper-bound moment ( $M_{up-bnd}$ ) are also labeled in the figure; these values will be discussed in  
174 the “Theoretical Comparison” section of this paper.

175

176 Both specimens exhibited similar behavior during testing. For both tests, the load response  
177 was initially linear-elastic until the pile lost stiffness due to cracking. Cracks were primarily  
178 vertical and were located within the constant moment region. The prestress force limited  
179 formation and growth of cracks at locations away from the splice, however, closer to the  
180 splice the full prestress force is not present, which allows crack initiation.

181

182 For both tests, peak load corresponded to crushing of the compression zone adjacent to the  
183 splice. The portion of the concrete that spalled away at peak load was outside of the  
184 transverse reinforcement that supported the core of the piles. Displacement at peak moments  
185 for Test 1 and Test 2 were 4.5 inches and 7.3 inches, respectively. Crushing occurred on the  
186 same side of the splice as the largest of the flexural cracks (Fig. 10). The additional  
187 displacement observed in Test 2 is attributed to the separation between the concrete and the  
188 splice assembly (Fig. 11).

189

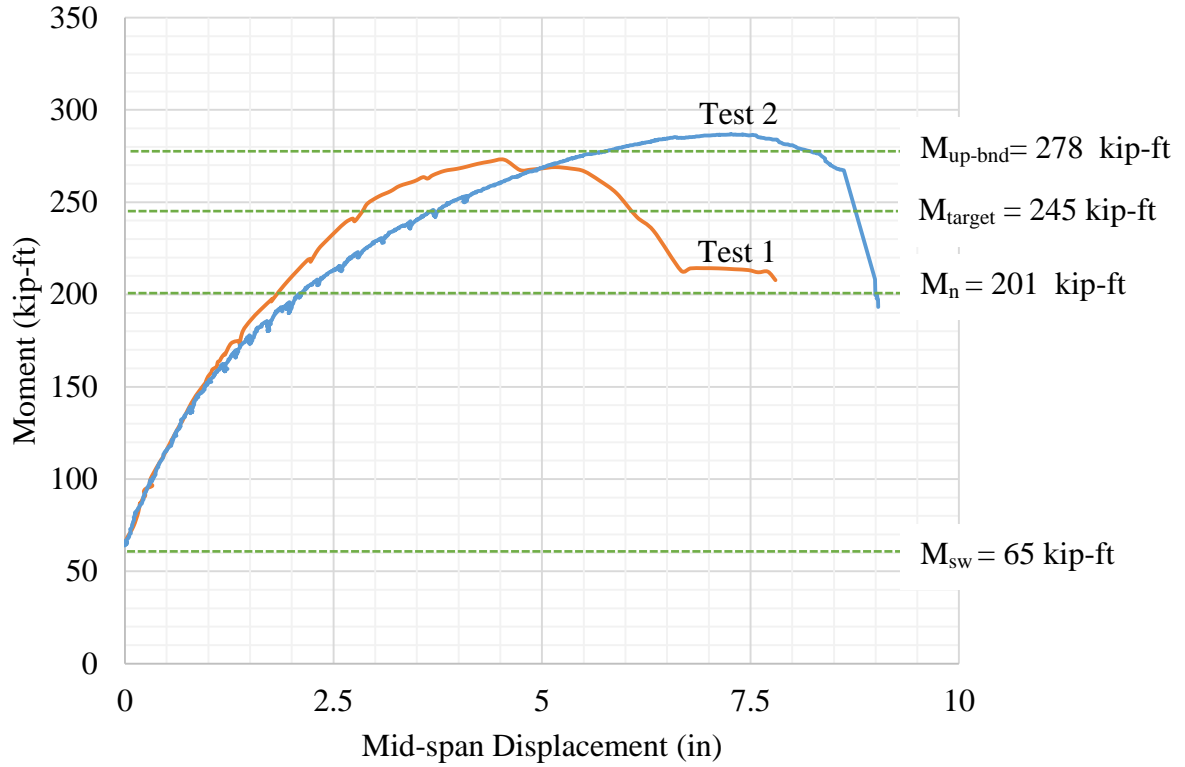
190 For Test 1, popping noises were heard as the test approached the peak moment. The noises  
191 seemed to come from the splice location, and are attributed to bending of the locking pins  
192 and separation of the splice assembly and #10 bars from the concrete. For both tests, the  
193 locking pins were initially centered in the holes, but testing caused permanent deformation of  
194 the pins towards the side of the holes (Fig. 12). Deformation was more obvious in the pins on  
195 the flexural-tension side.

196

197 The post-test width of the cracks adjacent to the splice in Test 1 and Test 2 (Fig. 10) were  
198 approximately 0.5”. The cracks were wider while the piles were under load; however, no  
199 measurements of crack width were taken during loading. The width and location of the crack  
200 indicate that the #10 bars and splice assembly did not maintain strain compatibility with the  
201 concrete at peak loads. Separation of the concrete and splice observed in Test 2 also supports  
202 this notion. Loss of strain compatibility is considered in the theoretical calculations presented  
203 in the next section.

204





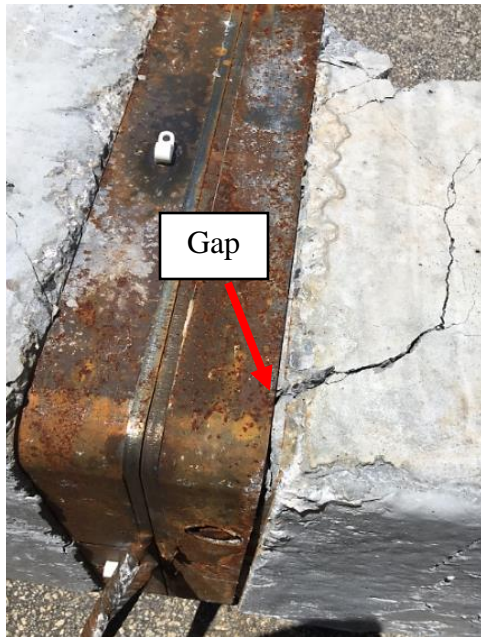
205  
206  
207  
208  
209

Fig. 9 – Moment-displacement response of piles



210  
211  
212

Fig. 10 – Failure of compression zone of Test 1 (left) and Test 2 (right)



213

214 Fig. 11- Gap between splice assembly and the concrete in Test 2

215



216

217 Fig. 12 – Test 1 location of locking pin prior to (left) and after (right) load tests

218

219

220 **THEORETICAL COMPARISON**

221

222 The experimental moment capacities of the splices were 273 kip–ft for Test 1 and 287 kip–ft  
 223 for Test 2. These values account for bending moments caused by self-weight and applied  
 224 load, and were calculated as:

225

$$M_{exp} = \frac{w_{sw}L^2}{8} + \frac{Pa}{2}$$

226

227 Table 3 – Values used for calculating loads

Variable	Definition	Value
$w_{sw}$	Uniform load from self-weight	0.337 klf
$L$	Span length	39.0 ft
$P$	Load applied by jack	28.5 kip at peak load for Test 1 30.3 kip at peak load for Test 2
$a$	Distance between load point and support	14.7 ft

228

229 The experimental moment capacity was compared to two different theoretical capacities: 1)  
 230 Nominal capacity using specified material properties, and 2) Upper-bound capacity using  
 231 ultimate material properties. These capacities are compared to the experimental results in  
 232 and summarized in Table 4. Comparisons are also made to the FDOT-required flexural  
 233 capacity ( $M_{target}$ ) of 245 kip-ft. The experimental capacity of both specimens exceeded the  
 234 FDOT-required capacity.

235

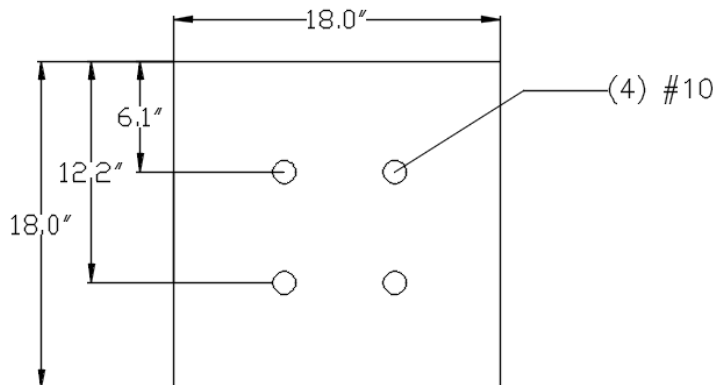
236 Table 4 - Comparison of theoretical and experimental bending moments

$M_{exp}$	$M_{exp}$	$M_n / M_{exp}$	$M_{up-bnd} / M_{exp}$	$M_{target} / M_{exp}$
Test 1	273 kip-ft	0.74	1.02	0.90
Test 2	287 kip-ft	0.70	0.97	0.85

Note:  $M_n = 201$  kip-ft,  $M_{up-bnd} = 278$  kip-ft

237

238 The #10 bars were designed to have the smallest tensile capacity of the components within  
 239 the splice system. Accordingly, the splice capacity was modeled using the reinforced  
 240 concrete section shown in Fig. 13. Prestressing strands were discontinuous at the splice  
 241 location and were not considered in the flexural capacity calculations.



242

243 Fig. 13 – Cross-section used for calculating flexural capacity

244

245 The nominal moment capacity ( $M_n$ ) was calculated based on the material properties specified  
 246 in the design documents provided by the splice and pile suppliers. Yield strength of #10 bars

247 was taken as 72 ksi, and the concrete compressive strength was taken as 6000 psi. The  
248 nominal capacity of 201 kip-ft was 26% and 30% lower than Test 1 and Test 2 experimental  
249 values, respectively. This result is attributed to the conservative values used for the material  
250 properties, and to the loss of bond between the lower #10 bars and the concrete. This loss of  
251 bond allowed the #10 bars to reach stress values much higher than the specified yield stress.  
252 Thus the nominal capacity provides a very conservative value for the flexural capacity of the  
253 pile splice.

254

255 The upper-bound capacity ( $M_{up-bnd}$ ) of the splice connection was based on tested material  
256 properties and on physical observations from testing. As such, the upper-bound capacity is  
257 intended to be a more accurate description of the experimental results than the nominal  
258 capacity. Details of the upper-bound calculations are shown in Fig. 14, and key concepts  
259 from the calculations are described below:

260

261 • The bottom #10 bars reached ultimate stress. The large crack observed behind the cap  
262 plate indicated that bond between the lower #10 bars and the concrete was lost at higher  
263 load levels. Accordingly, strain compatibility was not assumed for the bottom bars.  
264 Rather, stress in the bottom bars was assumed to equal the tested ultimate stress of 110  
265 ksi. This is the maximum possible stress that the bars could support, hence the resulting  
266 moment capacity is termed the “upper-bound” capacity.

267

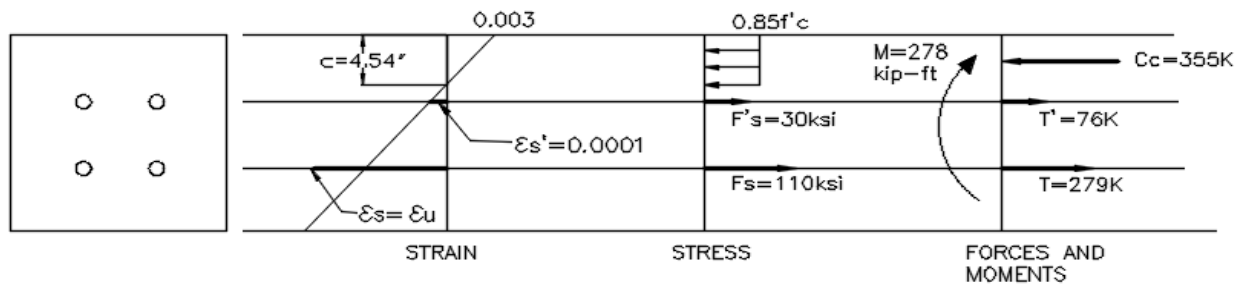
268 • Strain compatibility of top #10 bars. The crack behind the cap plate was much smaller at  
269 the level of the top bars and it is assumed that bond was maintained between the concrete  
270 and top bars. Stress in the top bars was determined using the constitutive relationship  
271 shown in Fig. 15. The figure is based on tested data for the #10 provided by the bar  
272 supplier. Stress in the top bars was calculated to be 30 ksi at the upper-bound capacity.

273

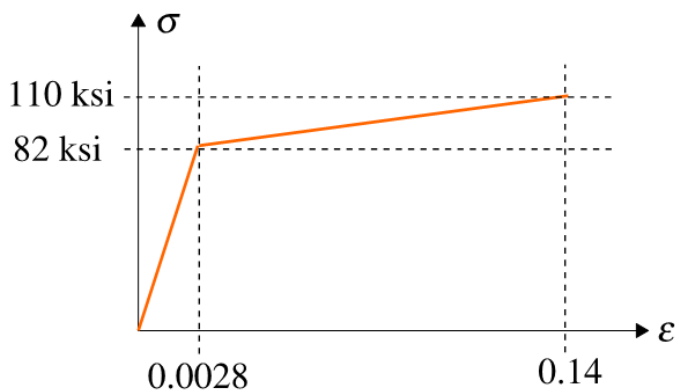
274 • Concrete compressive strength of 7700 psi. Test data provided by precaster shows that  
275 typical compressive strengths for the concrete mix used in the piles was approximately  
276 7700 psi at 28 days.

277

278 • Equilibrium. Force equilibrium is satisfied at a neutral axis depth of 4.54 in. This value  
279 is based on the approach and material properties described above, and the geometry  
280 shown in Fig. 13.



281  
282 Fig. 14 – Mechanics at ultimate capacity  
283



284  
285 Fig. 15 – Stress-strain relationship for top bars in upper-bound calculations  
286

287 The calculated upper-bound moment capacity is 278 kip-ft. This value is 2% larger than the  
288 experimental capacity of Test 1 and 3% lower than Test 2. This level of agreement suggests  
289 that the assumptions made in the upper-bound calculations are reasonable descriptions of the  
290 physical behavior of the splice at ultimate capacity. Thus it is concluded that the bottom bars  
291 were approaching ultimate stress when the concrete compression zone crushed.

292  
293

## 294 SUMMARY AND CONSLUSIONS

295

296 Tests were conducted to identify the flexural capacity of a splice connection for precast  
297 concrete piles. Two specimens were tested, each consisting of two 18 inch x 18 inch x 20  
298 foot pile segments. After positioning the segments end-to-end with a crane, the splice  
299 connections were completed within minutes. The resulting 40-foot long specimens were load  
300 tested in four-point bending to determine the flexural capacity of the splice connection. The  
301 connections exhibited experimental moment capacities of 273 kip-ft and 287 kip-ft for Test 1  
302 and Test 2, respectively. For both tests, peak moment corresponded to crushing of the  
303 concrete in the flexural compression.

304

305 Nominal and upper-bound flexural capacities were calculated for the splice connection. The  
306 nominal capacity was calculated based on specified material properties and was 201 kip-ft, or  
307 26% and 30% lower than the experimental capacities of Test 1 and Test 2, respectively. The  
308 upper-bound capacity was calculated using tested material properties and by assuming that  
309 the lower #10 bars were at ultimate stress. This assumption is supported by the observation  
310 made during testing that the concrete and splice assembly separated at higher loads. The  
311 separation indicated loss of bond (strain compatibility) between the #10 bars and the  
312 concrete, and allowed the bars to reach stresses much higher than the specified yield stress.  
313 The upper-bound capacity was 278 kip-ft, or 2% larger than the experimental capacity of  
314 Test 1 and 3% lower than the experimental capacity of Test 2. These results suggest that the  
315 lower #10 bars were near ultimate stress when the concrete compression zone crushed at  
316 peak load.

317

318 The Florida Department of Transportation requires that mechanical splice connections in 18  
319 inch x 18 inch piles have a flexural capacity of at least 245 kip-ft. Both of the splice  
320 specimens exceeded this value.

321

322

### 323 **ACKNOWLEDGEMENTS**

324

325 Testing and analysis were sponsored by Emeca/SPE-USA and Aver Technologies, Inc. The  
326 pile specimens were fabricated by Gulf Coast Pre-Stress.

327

### 328 **REFERENCE**

329

1. Florida Department of Transportation, *Standard Specification for Road and Bridge  
330 Construction*. 2015 Tallahassee, FL.

331

2. Florida Department of Transportation, *Design Standards Index No. 20618*.  
332 Tallahassee, FL.

333

334